Journal of Cluster Science (2022) 33:1427–1433
https://doi.org/10.1007/s10876-021-02070-z

ORIGINAL PAPER

Fabrication of Gallic Acid Loaded SeNPs and their Neuroprotection Effect for Treatment of Ischemic Stroke

Chao Lv[1] · Yan-Wei Chen[1] · Shu-Hui Dai[1] · Xiao-Fan Jiang[1] · Xia Li[1]

Received: 3 December 2020 / Accepted: 14 April 2021 / Published online: 24 April 2021

Abstract

Ischemic stroke (IS) is a usual cerebrovascular ailment having high mortality and morbidity globally. The approaches for the treatment and prevention of cerebral ischemia–reperfusion injury (CIRI) are very limited. In this study, a delivery system of selenium nanoparticles loaded with gallic acid (GA-SeNPs) was developed utilizing ascorbic acid (AA) as a reducing agent and gallic acid (GA) as a capping agent. In pharmacokinetic study, GA-SeNPs clearly increases the AUC of the plasma concentration–time and extended GA half-life. In vitro effects of GA-SeNPs in the middle cerebral artery occlusion (MCAO) model and the oxygen glucose deprivation (OGD) model was measured. Finally, GA-SeNPs can be utilized as an efficient vehicle for delivery of GA in CIRI treatment.

Keywords Selenium nanoparticles · CIRI · Gallic acid

Introduction

Cerebral stroke has proved to be the most critical condition among various health issues [1]. Currently, in depth research is running to understand the mechanism and dynamics of disease, treatment for stroke along with its related disabilities and development of preventive approaches [2, 3]. A challenging task for industry as well as pharmaceutical sciences is to develop central nervous system (CNS) targeting drugs. Poor delivery through blood–brain barrier (BBB), fast metabolism and elimination from the systemic circulation hinder the effectiveness of most CNS drugs [4]. The development of anti-stroke drugs is a big challenge because of its difficulty in signaling process and corresponding inflammatory response which complicates the disease. Signaling networks in mammalian CNS such as Jak-Stat, Hippo-Yap-Mst, Wnt/β-Catenin, mTOR affect the neuronal metabolism and growth [5, 6], hence dysregulation of signaling network pathways during the stroke and after the stroke causes neuronal cell damage which leads to death [7]. Pro-inflammatory cytokines inhibit memory consolidation, hippocampal neurogenesis and synaptic plasticity [8]. By having sound knowledge over these pathways helps in rational targeting of specific pathways which results in effective therapeutic approaches with less side effects. An intense research is ongoing for the development of NP- based approaches in drug release and targeted therapy [9, 10].

To discover potentially efficient compounds against cerebral ischemia–reperfusion injury (CIRI), great attempts are being made from past few years. Enormous studies have revealed that plant nutrients or polyphenols like GA, resveratrol and corilagin are effective in the prevention of IS because of their antioxidant and anti-inflammatory effects [11–13]. GA is broadly distributed in naturally available nutrients along with many common herbs and fruits. Therefore it can be used in the treatment and prevention of IS because of the huge possibilities in its application and development. Besides being an active

✉ Xia Li
sjwklixia@sina.com; xiali16@yahoo.com

Chao Lv
be_way@163.com

Yan-Wei Chen
chen_yw888@126.com

Shu-Hui Dai
dsh20012004@163.com

Xiao-Fan Jiang
jiangxf@fmmu.edu.cn

[1] Department of Neurosurgery, The First Affiliated Hospital of Airforce Medical University, Xi'an 710000, Shaanxi, China

molecule, GA also has a simplest form of chemical structure among the naturally obtained polyphenol compounds [13]. From previous studies it is evident that GA has the capability to increase the antioxidant and anti-inflammatory capacity of the brain [14–16]. In case of cardiovascular and cerebral diseases, GA has been considered as an assuring therapeutic polyphenol, although its pharmacokinetic characteristics like, poor bioavailability, low absorption along with rapid elimination, were reported to be the main bottlenecks in clinical practice [17]. To resolve such complications in drug delivery system, a new technique known as encapsulation has evolved as a most successful method for some drugs. Furthermore, SeNPs were exploited for targeting brain drug delivery systems. Literature studies have showed the use of water-soluble O-carboxymethyl chitosan (O-CMC) loaded with boswellic acid for its effect in a brain injury model [18]. Similarly, biomolecules such as Quercetin [19], Eugenol [20], glycyrrhizic-acid [21] and Naringenin [22] were surface modified or loaded onto nanoparticles or made nanoformulations for use in treatment of cerebral ischemia. Thus, we assumed that the prepared GA- SeNPs can likely increase the effectiveness of GA against the condition of CIRI.

In this study, a delivery system of selenium nanoparticles loaded with gallic acid (GA-SeNPs) was developed utilizing ascorbic acid (AA) as a reducing agent and gallic acid (GA) as a capping agent. In pharmacokinetic study, GA-SeNPs clearly increases the AUC of the plasma concentration–time and extended GA half-life. In vitro effects of GA-SeNPs in the middle cerebral artery occlusion (MCAO) model and the oxygen glucose deprivation (OGD) model was measured.

Materials and Methods

Synthesis of Selenium Nanoparticles

In the current study, we described the environmentally friendly fabrication of GA-SeNPs by mixing 1 mL of 50 mM GA with 30 mM selenious acid (10 mL) in the presence of 40 mM ascorbic acid (1 mL), which was utilized as a reduction reaction initiator. The UV–Vis spectroscopic results after 24 h of reaction showed the formation of GA-SeNPs. The mixture was then subjected to centrifugation for about half an hour at 10,000 rpm following 24 h of incubation. Double distilled water (DDW) was utilized to wash the resultant pellet followed with absolute ethanol for three times. The obtained pellet was then dried overnight. Ultra-sonification was utilized to subject the red GA-SeNPs powder in PBS of 7.4 pH, followed by centrifugation.

Drug Loading Efficiency (LE) and Entrapment Efficiency (EE)

The loading efficiency (LE) and entrapment efficiency (EE) of GA-SeNPs were calculated with the help of HPLC method as described earlier [23]. The UHPLC–MS/MS instrument containing Accela 1250 UHPLC system fixed with a Thermo Fisher Scientific Inc., Waltham, MA, USA, TSQ quantum ultra-triple-quadrupole mass spectrometer. A Phenomenex Kinetex XB-C18 column (2.1 × 150 mm, 1.7 μm) was used for Chromatographic separations. The mobile phase was prepared by mixing water having 0.1% formic acid (A) and acetonitrile with 0.1% formic acid (B). The gradient elution was conducted as follows: 0–3.0 min, 2% B; 3.0–10.0 min, 10% B; 10.0–17.0 min, 2% B. On the other hand, the temperature of column was sustained to be at 251 °C. The injection volume and the flow rate were maintained to be 5 μL and 200 μL/min, successively. Methanol was used for needle wash after each injection. On comparing with the amount of drug received initially, EE was calculated as percentage of GA obtained from the GA-SeNPs. LE was expressed as the quantity of entrapped GA in comparison to that of the total GA-SeNPs.

By using dialysis bags, the GA released in vitro from the GA-SeNPs was demonstrated. These GA-SeNPs were kept in pretreated dialysis sacs which were then immersed in PBS (pH 7.4) of 100 mL volume to undergo mechanical agitation at a temperature of 37 °C. At frequent time periods, the withdrawal and restoration of the same medium was done. All these parameters were taken thrice while performing the experiments.

Pharmacokinetics

All the animal experiments and protocols were performed with the approval from Institutional Animal Experiment Ethics Committee of the First Affiliated Hospital of Airforce Medical University, China. To conduct a pharmacokinetic experiment, rats were separated equally into two groups. One group was subjected to GA treatment and another group was treated with GA-SeNPs while the number of rats in each group were eight. The oral administration of GA-SeNPs (consisting of GA 50 mg/kg) in a saline solution and native GA (50 mg/kg) dispersed in solution of CMC-Na (0.5%, w/v) was done. The dosage chosen was based on previously performed studies on GA [24, 25]. We collected blood samples via the caudal vein at predetermined point of time. On centrifugation, the serum was obtained and then stored at temperature of − 80 °C for future use. With the help of a liquid chromatographic system, Agilent 1100 provided with a reversed-phase column, the content of GA was determined. The

pharmacokinetic parameters in a noncompartmental model were calculated using WinNonlin 6.2. By extrapolating trapezoidal rule to infinity, the AUC (area under plasma concentration time curve) was determined. The systemic clearance (Cl) and terminal elimination half-life ($t_{1/2}$) were determined.

Oxygen–Glucose Deprivation and Reoxygenation

To understand the GA-SeNPs in vitro effects upon CIRI, OGD model was employed. As described earlier, cortical nerves were taken from the brains of 24 h old rats [26]. These were cultured at room temperature (37 °C) in a humidified atmosphere with 5% CO_2. To maintain, in vitro ischemic conditions, the primary cultured cortical neurons were subjected to temporary OGD for a duration of 60 min. Later, they were incubated in a 5% air box containing CO_2 for a day. To simulate the deficiency of blood in vitro, five groups were designed which were OGD group, OGD + GA group (50 μM in DMSO with dose decision made from previous studies) [27], control group (no OGD), OGD + GA-SeNPs group and OGD + void NPs group. Using the medium-treated cells as controls, the DMSO concentration into cultured medium remained $< 0.1\%$ w/v.

The cell viability was determined by MTT analysis in every group as reported earlier [28]. The lactate dehydrogenase (LDH) release was identified with the help of commercially available kit. The data was conveyed in the form of percentage (%) of control levels.

Characterization

The formation of SeNPs was known by using a double beam Shimadzu, UV-1800, Ultraviolet-visual (UV–Vis) spectrophotometer. The absorption measurements were performed within the wavelength range of 200–500 nm. To know the morphology, shape and size of NPs, about 1 mL of the nano colloid was dropped on copper grids which is carbon-coated, followed by air dried, and studied under transmission electron microscope (TEM, JEM 1400) at 100 kV. Further the Fourier transform infrared spectroscopy (FTIR) analysis was performed by preparing pellet of NPs with KBr powder, which later used for measurements using Nicolet 6700 spectrometer FTIR instrument, (Thermo Electron Corporation, USA) at 4 cm^{-1}. An X-ray diffraction (X′Pert Pro PANalytical, ALMELO, Netherlands) instrument was utilized to know the structural characterization of prepared SeNPs. XRD measurements were performed with 2θ range from 0° to 80° at a voltage of 45 kV using 40 mA current.

Statistical Analysis

The statistical analysis was performed by using statistical package for social sciences (SPSS) version 19.0 software. Excluding the scores of neurological deficits, the remaining data was expressed in the form of average ± standard deviation (SD).

Results and Discussion

Characterization of Prepared NPs

The formation of GA-SeNPs using ascorbic acid mediated reduction and gallic acid attachment is represented (Scheme 1). Figure 1 showed the UV–Vis absorption of reaction mixture of gallic acid and Selenous acid mixture at 0 h and after 24 h. The study of UV–Vis spectroscopy indicated the green synthesis of GA-SeNPs from Selenous acid which was also visually known by change in color to red (Shown in Fig. 1 inset) from colorless selenium acid with a maximum absorption at 261 nm (λmax). This change in color is due to the surface plasma resonance (SPR) absorption of SeNPs. On the other hand, the optical absorption of reaction mixture at 0 h is found to be 282 nm which is because of UV–Visible absorption of gallic acid, which is blue shifted and a new broad peak at 261 appeared indicated the formation of SeNPs (Fig. 1).

Figure 2 demonstrated the size and morphology of the fenugreek-synthesized NPs. The shape of the GA-SeNPs fabricated was found to be spherical as shown in TEM images. Particles are found to be crystalline with the particle size of about 50–60 nm.

The XRD technique was utilized to determine the phase composition as well as crystal structure of the GA-SeNPs as represented in Fig. 3. XRD pattern confirms the nature of the sample as nanocrystalline, which is well in accordance with the regular Se powder, thus indicates the production of GA-SeNPs. The determined lattice constant values are c = 4.952 A° and a = 4.363 A°, these values are corresponding with the results of earlier literature (JCPDS File No: 06-0362).

Figure 4 displays the FTIR spectra of GA-SeNPs, which are obtained by the reduction of GA. The existence of narrow and strong peak at 1702 cm^{-1} and the strong, broad band between 3600 and 2500 cm^{-1} regions could be allocated to carbonyl and OH group stretching vibrations, which indicates the presence of carboxyl group. The three different peaks are noticed at 1450, 1616, 1541 cm^{-1} are the typical C–C bond stretching vibrations of an aromatic ring. There are many peaks appeared in between 1300 and 1000 cm^{-1}, which are allocated to the O–H bond bending

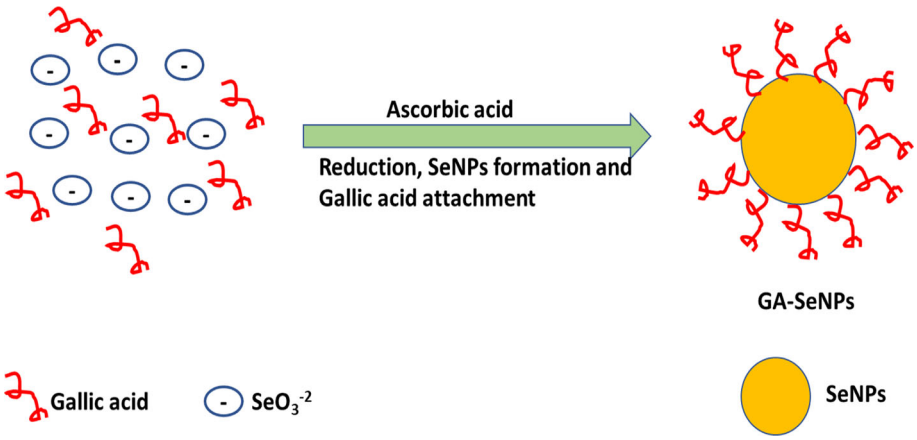

Scheme 1 Schematic representation of preparation of GA-SeNPs

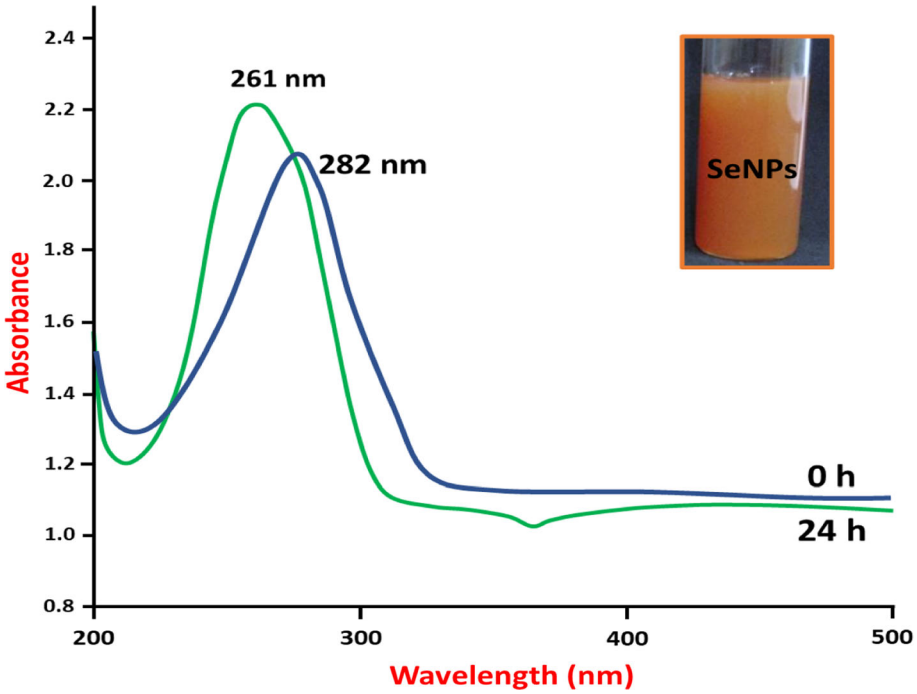

Fig. 1 UV–Visible absorbance spectrum of GA + SeNPs at 0 h (green) and 24 h (blue) (color figure online)

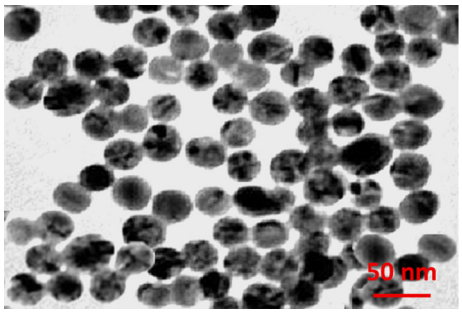

Fig. 2 TEM image of synthesized selenium nanoparticles

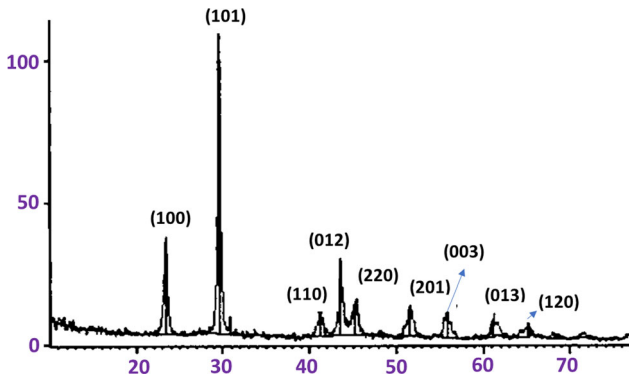

Fig. 3 XRD pattern GA-SeNPs

vibrations and C–O bond stretching vibrations of GA. Further, the presence of these peaks corresponding to oxygen functionalities such as O–H bond, carbonyl group stretching, and C–C bond stretching vibrations of an aromatic ring indicated the gallic acid loading onto SeNPs.

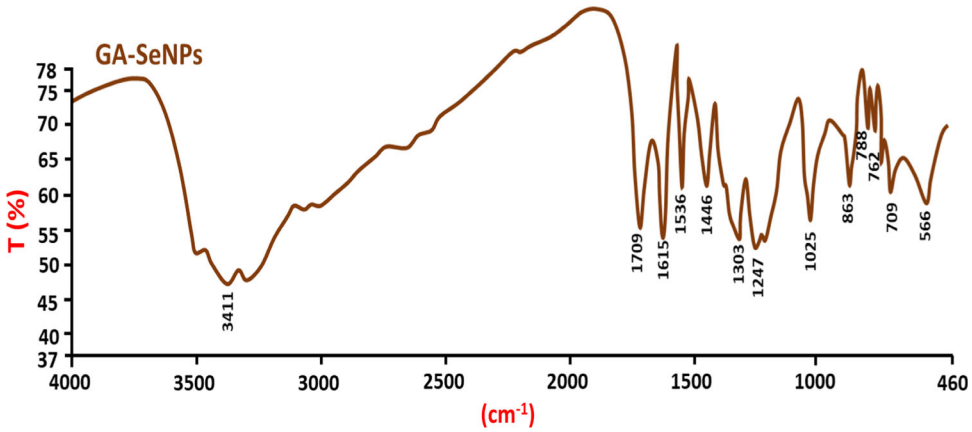

Fig. 4 FTIR spectra of GA-SeNPs

In vitro release curve of GA-SeNPs was explained in Fig. 5. GA-SeNPs explained that 50% of drug was released in original 6 h solution with decelerate, constant release rate. After four days, the quantity of released drug was increased by more than 70%. The initial quantity of drug released which was observed due to the segregation of surface absorption of GA-SeNPs in polymer matrix.

Pharmacokinetics (PK) of GA-SeNPs

The curves of plasma concentration–time for GA-SeNPs and GA on oral administration was explained in Fig. 6. Table 1 shows the pharmacokinetic parameters of GA-SeNPs. The plasma area under the curve (AUC) of GA-SeNPs (13.8 mg min/mL) was increased when compared to GA (5.2 mg min/mL) (p is less than 0.05). The gradual release of GA in the NP system enhances the circulation half-life ($t_{1/2}$) and AUC of GA (p is less than 0.05).

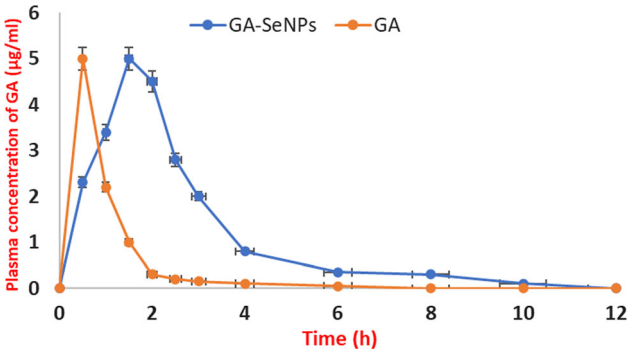

Fig. 6 The plasma concentration–time curves after administration of GA and GA-SeNPs (n = 8). *$p < 0.05$ vs. GA group

Protection of the Nerve Cells by GA-SeNPs from Oxygen–Glucose Deprivation-Induced Injury

The cell viability of 5 groups as showed in Fig. 7. In the treatment groups of OGD, the cell apoptosis proportion was 75% approximately. We did not observe any

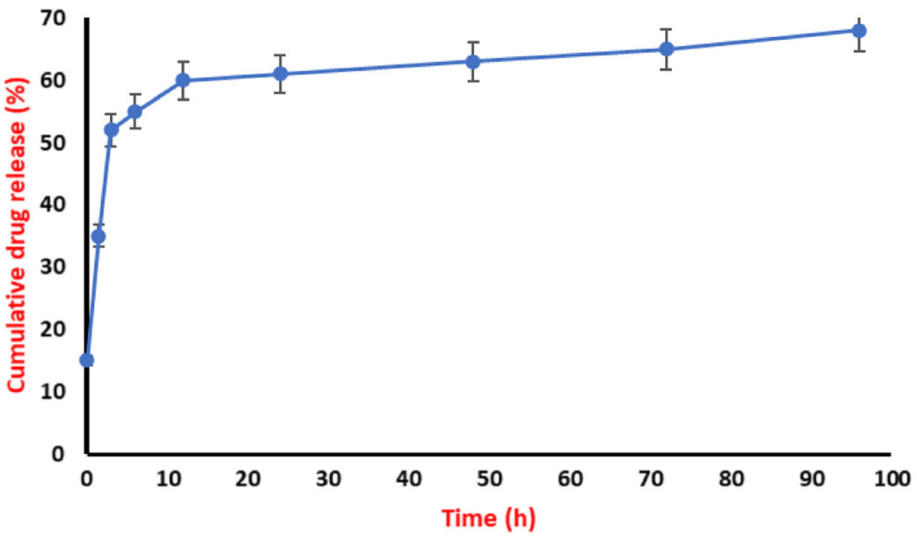

Fig. 5 In vitro release profile of GA from the GA-SeNPs

Table 1 Physiologic parameters of rats at pre-ischemia and 90 min after reperfusion

	Blood glucose (Glu) (mg/dl)	Arterial oxygen tension (PaO_2) (mm Hg)	Arterial carbon dioxide tension ($PaCO_2$) (mm Hg)	pH	Mean arterial blood pleasure (mm Hg)
90 min after reperfusion					
GA-SeNPs	142.9 ± 13.2	137.4 ± 12.8	38.2 ± 8.9	7.29 ± 0.16	112.3 ± 6.9
GA	148.3 ± 15.9	143.2 ± 10.9	38.8 ± 7.6	7.28 ± 0.13	105.6 ± 6.2
SeNPs	138.9 ± 14.8	138.2 ± 9.8	37.6 ± 5.2	7.40 ± 0.20	96.3 ± 6.9
Vehicle	148.5 ± 10.1	131.9 ± 9.5	36.8 ± 5.8	7.28 ± 0.25	103.7 ± 7.2
Sham	143.1 ± 8.3	137.8 ± 16.6	33.9 ± 4.0	7.32 ± 0.10	107.2 ± 9.8
Pre-ischemia					
GA-SeNPs	132.8 ± 9.2	149.2 ± 14.8	35.9 ± 4.2	7.29 ± 0.06	113.8 ± 5.8
GA	140.9 ± 10.2	147.2 ± 12.9	41.8 ± 3.4	7.42 ± 0.20	106.3 ± 6.9
SeNPs	130.8 ± 12.2	139.3 ± 14.4	40.1 ± 2.9	7.65 ± 0.15	110.9 ± 8.2
Vehicle	137.6 ± 11.3	146.6 ± 13.4	41.5 ± 4.5	7.25 ± 0.20	119.5 ± 4.1
Sham	139.9 ± 9.0	156.5 ± 16.2	40.4 ± 5.0	7.05 ± 0.89	116.4 ± 8.1

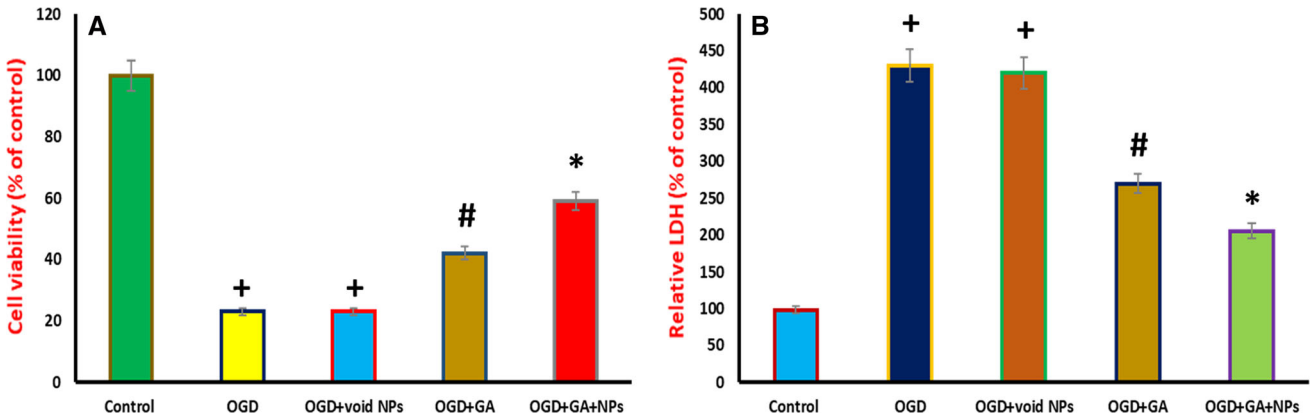

Fig. 7 Effects of GA-SeNPs on cell viability (**a**) and LDH release (**b**) in a primary culture of rat cortical neurons exposed to OGD. Data showed means ± Standard Deviation and the experiments were performed thrice. *$p < 0.05$ vs. OGD + GA; #$p < 0.05$ vs. OGD group; + $p < 0.05$ vs. control

considerable changes in the survival rate of the cell between OGD group and NP group (p greater than 0.05). Cell viability of OGD group i.e. (45 ± 3%) was less then GA-SeNPs group (60 ± 5%) as showed in Fig. 7 (p is less than 0.05). The protective effects of GA-SeNPs were confirmed by LDH testing and showed that the treatment of GA-SeNPs has decreased the release of OGD-induced lactate dehydrogenase (LDH) by 47% approximately (p is less than 0.05) (Fig. 7). In order to evaluate cytotoxicity, MTT assay was used to evaluate cell viability after exposing to GA-SeNPs for about 2 days (1–100 μM), and there was no significance noticed between the control and treated groups (data not shown).

Conclusions

In conclusion, a delivery system of Se NPs loaded with gallic acid was developed utilizing ascorbic acid as a reducing agent and gallic acid as a capping agent for its synthesis. In pharmacokinetic study, GA-SeNPs clearly increase the AUC of the plasma concentration–time and extended GA half-life. In vitro effects of GA-SeNPs in the middle cerebral artery occlusion model and the oxygen glucose deprivation model was measured. Finally, GA-SeNPs can be utilized as an efficient vehicle for delivery of GA in CIRI treatment.

References

1. U. Chamorro, X. Dirnagl, and A. M. Urra (2016). *Lancet Neurol.* **15**, 869–881.
2. H. Amani, E. Mostafavi, H. Arzaghi, S. Davaran, A. Akbarzadeh, O. Akhavan, H. Pazoki-Toroudi, and T. J. Webster (2018). *ACS Biomater. Sci. Eng.* **5**, 193–214.
3. N. Ghadernezhad, L. Khalaj, H. Pazoki-Toroudi, M. Mirmasoumi, and G. Ashabi (2016). *Pharm. Biol.* **54**, 2211–2219.
4. H. Amani, R. Habibey, S. J. Hajmiresmail, S. Latifi, H. Pazoki-Toroudi, and O. Akhavan (2017). *J. Mater. Chem. B* **5**, 9452–9476.
5. R. A. Saxton and D. M. Sabatini (2017). *Cell* **168**, 960–976.
6. H. Pazoki-Toroudi, H. Amani, M. Ajami, S. F. Nabavi, N. Braidy, P. D. Kasi, and S. M. D. Nabavi (2016). *Ageing Res. Rev.* **31**, 55–66.
7. M. Ajami, H. Pazoki-Toroudi, H. Amani, S. F. Nabavi, N. Braidy, R. A. Vacca, A. G. Atanasov, A. Mocan, and S. M. D. Nabavi (2017). *Neurosci. Biobehav. Rev.* **73**, 39–47.
8. A. Borsini, P. A. Zunszain, S. Thuret, and C. M. Pariante (2015). *Trends Neurosci.* **38**, 145–157.
9. A. Gaudin, M. Yemisci, H. Eroglu, S. Lepetre-Mouelhi, O. F. Turkoglu, B. Dönmez-Demir, S. Caban, M. F. Sargon, S. Garcia-Argote, G. Pieters, O. Loreau, B. Rousseau, O. Tagit, N. Hildebrandt, Y. Leantec, J. Mougin, S. Valetti, H. Chacun, V. Nicolas, D. Desmaële, K. Andrieux, Y. Capan, T. Dalkara, and P. Couvreur (2014). *Nat. Nanotechnol.* **9**, 1054.
10. X. Zeng, M. Luo, G. Liu, X. Wang, W. Tao, Y. Lin, X. Ji, L. Nie, and L. Mei (2018). *Adv. Sci.* **5**, 1800510.
11. J. Abraham and R. W. Johnson (2009). *Rejuvenation Res.* **12**, 445–453.
12. Y. Ding, D. Ren, H. Xu, W. Liu, T. Liu, L. Li, J. Li, Y. Li, and A. Wen (2017). *Oncotarget* **8**, 114816.
13. M. Daglia, A. Di Lorenzo, S. F. Nabavi, Z. S. Talas, and S. M. Nabavi (2014). *Curr. Pharm. Biotechnol.* **15**, 362–372.
14. M. S. Korani, Y. Farbood, A. Sarkaki, H. F. Moghaddam, and M. T. Mansouri (2014). *Eur. J. Pharmacol.* **733**, 62–67.
15. A. Sarkaki, Y. Farbood, M. K. Gharib-Naseri, M. Badavi, M. T. Mansouri, A. Haghparast, and M. A. Mirshekar (2015). *Can. J. Physiol. Pharmacol.* **93**, 687–694.
16. M. T. Mansouri, Y. Farbood, M. J. Sameri, A. Sarkaki, B. Naghizadeh, and M. Rafeirad (2013). *Food Chem.* **138** (2–3), 1028–1033.
17. J. Sun, Y. Z. Li, Y. H. Ding, J. Wang, J. Geng, H. Yang, J. Ren, J. Y. Tang, and J. Gao (2014). *Brain Res.* **1589**, 126–139.
18. Y. Ding, Y. Qiao, M. Wang, H. Zhang, L. Li, Y. Zhang, J. Ge, Y. Song, Y. Li, and A. Wen (2016). *Mol. Neurobiol.* **53**, 3842–3853.
19. N. Ahmad, R. Ahmad, A. A. Naqvi, M. A. Alam, R. Abdur Rub, and F. J. Ahmad (2017). *Drug Res. (Stuttg)* **67**, 564–575.
20. N. Ahmad, R. Ahmad, M. A. Alam, and F. J. Ahmad (2018). *Drug Res. (Stuttg)* **68**, 584–595.
21. N. Ahmad, A. M. Al-Subaiec, R. Ahmad, S. Sharma, M. A. Alam, M. Ashafaq, R. A. Rub, and F. J. Ahmad (2019). *Artif. Cells Nanomed. Biotechnol.* **47**, 475–490.
22. N. Ahmad, R. Ahmad, F. J. Ahmad, W. Ahmad, M. A. Alam, M. Amir, and A. Ali (2020). *Saudi J. Biol. Sci.* **27**, 500–517.
23. F. Ma, X. Gong, X. Zhou, Y. Zhao, and M. Li (2015). *J. Ethnopharmacol.* **162**, 377–383.
24. Y. Konishi, Y. Hitomi, and E. Yoshioka (2004). *J. Agric. Food Chem.* **52**, 2527–2532.
25. S. Maya, T. Prakash, and K. Madhu (2018). *Neurochem. Int.* **121**, 50–58.
26. E. Pouresmaeili-Babaki, S. Esmaeili-Mahani, M. Abbasnejad, and H. Ravan (2018). *Rejuvenation Res.* **21**, 162–167.
27. O. Çimen, F. K. Çimen, M. Gülapoğlu, A. O. Bilgin, A. B. Çekiç, H. Eken, Z. Süleyman, Y. Bilgin, and D. Altuner (2018). *Biochem. Histopathol. Eval. Acta Cirurgica Bras.* **33**, 259–267.
28. Y. Ding, M. Chen, M. Wang, Y. Li, and A. Wen (2015). *Mol. Neurobiol.* **52**, 1430–1439.